

# Fabrication and Mechanical Properties of 5 Vol% Copper Dispersed Alumina Nanocomposite

Sung-Tag Oh,\* Tohru Sekino and Koichi Niihara

The Institute of Scientific and Industrial Research, Osaka University, 8-1 Mihogaoka, Ibaraki, Osaka 567, Japan

(Received 24 February 1997; accepted 18 April 1997)

## Abstract

*An optimum route to fabricate the  $Al_2O_3/Cu$  nanocomposite with sound microstructure and desired mechanical properties was investigated. Two methods for developing a uniform dispersion of Cu particles in  $Al_2O_3$  were compared on the basis of the resulting microstructures and mechanical properties. SEM and TEM analyses for the composites fabricated by reduction and sintering process using  $Al_2O_3/CuO$  powder mixture showed that the nano-sized Cu particles were well distributed and situated on the grain boundaries of the  $Al_2O_3$  matrix. The composite, hot-pressed at  $1450^\circ C$ , exhibited the maximum fracture strength and enhanced toughness compared with monolithic  $Al_2O_3$ . The strengthening was mainly attributed to the refinement of  $Al_2O_3$  matrix grains. The toughening mechanism in  $Al_2O_3/Cu$  composite was discussed by the observed microstructural features and theoretical predictions based on crack bridging model and thermal residual stress effect. Published by Elsevier Science Limited.*

## 1 Introduction

Niihara and his coworkers<sup>1–3</sup> have introduced a new concept of composites that have displayed the uniquely enhanced mechanical properties through the incorporation of nano-sized second phase within the matrix grains. These nanocomposites have also shown great potential for application to functional materials such as electromagnetic components, sensors and solid electrolyte from the viewpoint of cost effective solutions to the toughness or mechanical reliability problem.<sup>4,5</sup>

\*To whom correspondence should be addressed at Nano-Structure Processing Group, Synergy Ceramics Laboratory, FCRA, 1-1 Hirate-Cho, Kita-Ku, 462 Nagoya, Japan.

In this regard, new types of ceramic/metal nanocomposites such as  $Al_2O_3/W$ ,<sup>6</sup>  $Al_2O_3/Mo$ ,<sup>7</sup>  $Al_2O_3/Ni$ ,<sup>8</sup>  $ZrO/Mo$ ,<sup>9</sup> and  $BaTiO_3/Ni$ <sup>10</sup> have been successfully developed. The mechanical properties of these nanocomposites were notably enhanced by the dispersion of the nano-sized metal particles into the matrix grains. However, if the large metal particles, originating from as received metal powders and/or agglomerations during sintering existed in the matrix grain boundary, the advantages of the enhanced mechanical properties easily disappeared.<sup>6</sup> Particularly in the case of a ceramic/metal system composed of a metal phase with low-melting point, where the deterioration effect of mechanical properties will be seriously increased, due to the formation of large metal phases at grain boundaries or triple points, by the rapid diffusion of metal existing as a liquid phase during sintering. To obtain the desired mechanical properties, therefore, exact control of the microstructure is prerequisite.

$Al_2O_3$  and Cu (melting point of  $1084^\circ C$ ) were selected for the matrix and metal dispersions, respectively. Starting with two powder mixtures of  $Al_2O_3/Cu$  or  $Al_2O_3/CuO$  produced by milling and mixing, a reduction and sintering process, in hot-pressing, was used to obtain  $Al_2O_3/5$  vol% Cu composites. In this paper, the dependence of fabrication processes on microstructure and mechanical properties is described. Also, the toughening and strengthening mechanisms due to the addition of Cu particulates into the  $Al_2O_3$  matrix are analyzed based on the observed microstructure and theoretical prediction.

## 2 Experimental Procedures

Starting mixtures were prepared from the following powders:  $\alpha-Al_2O_3$  (99.95%,  $0.2 \mu m$ , Sumitomo

Chemical Co.) and either 5 vol% Cu metal powder (99.99%, 1  $\mu\text{m}$ ) or CuO powder (99.9%, 1–2  $\mu\text{m}$ ) corresponding to 5 vol% Cu, produced by High Purity Chemicals Lab. These powder mixtures were wet ball-milled in highly pure ethanol for 24 h using a polyethylene pot with high purity  $\text{Al}_2\text{O}_3$  balls. The milled powder mixtures were dried in an oven, and dry ball-milled for 24 h to avoid agglomeration.

The powder mixtures of  $\text{Al}_2\text{O}_3$  and CuO were reduced and sintered by a procedure similar to that reported by Sekino *et al.*<sup>6</sup> The mixtures were put into a graphite die and reduced at 350 and 1000°C for 30 min in  $\text{H}_2$  atmosphere, and consecutively the hot-pressing was carried out at 1400–1600°C for 1 h in Ar atmosphere under a pressure of 30 MPa. The heating rate of hot-pressing was 30°C  $\text{min}^{-1}$ . This procedure was also used for mixtures prepared by adding elemental Cu powder to  $\text{Al}_2\text{O}_3$ .

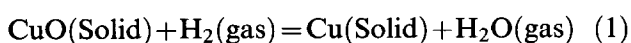
The hot-pressed bodies were cut, ground with a diamond wheel and polished using diamond pastes. The final diamond lap had an abrasive particle size of 0.5  $\mu\text{m}$  before fracture strength testing, the specimen edges were slightly beveled on the 1200-grit emery paper to remove notches introduced during grinding. The dimensions of all specimens tested in this investigation were 3×4×37 mm. The fracture strength was evaluated using a 3-point bending test with span 30 mm and cross-head speed 0.5 mm  $\text{min}^{-1}$ . The fracture toughness was measured by indentation fracture (IF) method with Vickers' hardness tester (98 N-load applied for 15 s.). The Young's modulus was determined by the resonance-vibration method using the 1st-mode resonance.

Phase identification of the composite was determined by X-ray diffraction analysis. The densities of the sintered samples were measured using Archimedes' principle in toluene, and the theoretical density was calculated by the law of mixtures. The microstructure was observed by SEM and more detailed by TEM. The grain sizes were estimated from the measurements of above 500 grains which were selected from four or more SEM micrographs of specimens thermally etched at 1400°C for 15 min.

### 3 Results and Discussion

#### 3.1 Reduction of CuO

The chemical reaction for the reduction of CuO by  $\text{H}_2$  gas can be represented as



Humidity curves for the hydrogen reduction process of the  $\text{Al}_2\text{O}_3/\text{CuO}$  powder mixture during heat-up to 1000°C with a heating rate of 10°C  $\text{min}^{-1}$  are presented in Fig. 1. Sharp increases in humidity curve were observed at 100 and 232°C, respectively. After these increases the curve decreased slowly to a temperature of approx. 750°C and then remained at the same value.

The first peak was for the evaporation of water in powder mixture and the second peak resulted from the water vapor formation by reduction of CuO as in eqn (1). Thus, the temperature for the second peak appears to be a reduction temperature of CuO in the present system and coincides with the reported reduction temperature of CuO.<sup>11</sup>

Figure 2 shows the X-ray diffraction pattern of the  $\text{Al}_2\text{O}_3/\text{CuO}$  powder mixture reduced at 1000°C in  $\text{H}_2$  atmosphere. As shown in the figure, in the region of XRD-resolution, the powder mixture was composed entirely of  $\text{Al}_2\text{O}_3$  and elemental Cu. This result agreed with that of the hygrometry measurement in Fig. 1. On the basis of this result, the reduction and sintering schedule of  $\text{Al}_2\text{O}_3/\text{CuO}$  powder mixture in hot-pressing was established.

#### 3.2 Effect of starting powder mixtures

To analyze an effect of initial powder mixtures on the composite properties, the prepared powder mixtures of  $\text{Al}_2\text{O}_3$  and either elemental Cu or CuO were hot-pressed at 1600°C for 1 h followed by the schedule mentioned in experimental procedure.

Typical fracture surfaces of hot-pressed composites prepared from  $\text{Al}_2\text{O}_3/\text{Cu}$  and  $\text{Al}_2\text{O}_3/\text{CuO}$  powder mixture are shown in Fig. 3(a) and (b), respectively. As clearly seen from Fig. 3(a), the large Cu particles and coarse  $\text{Al}_2\text{O}_3$  grains in the hot-pressed composite were observed. Conversely, the composite using  $\text{Al}_2\text{O}_3/\text{CuO}$  powder mixture exhibited a homogeneous dispersion of fine Cu particles and finer matrix grain size.

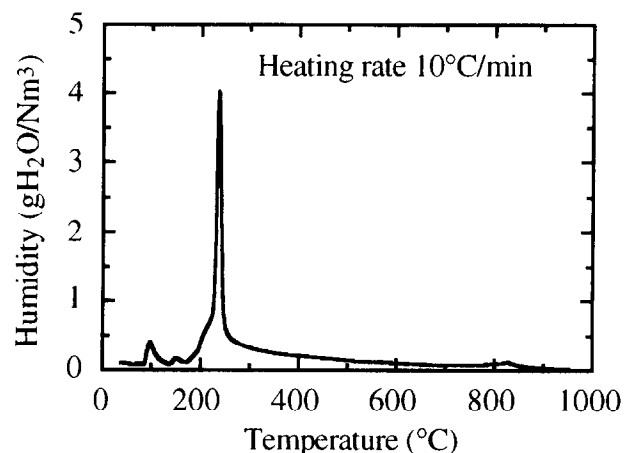


Fig. 1. Humidity curve for the hydrogen reduction of the  $\text{Al}_2\text{O}_3/\text{CuO}$  powder mixture during heat-up to 1000°C with the heating rate of 10°C  $\text{min}^{-1}$ .

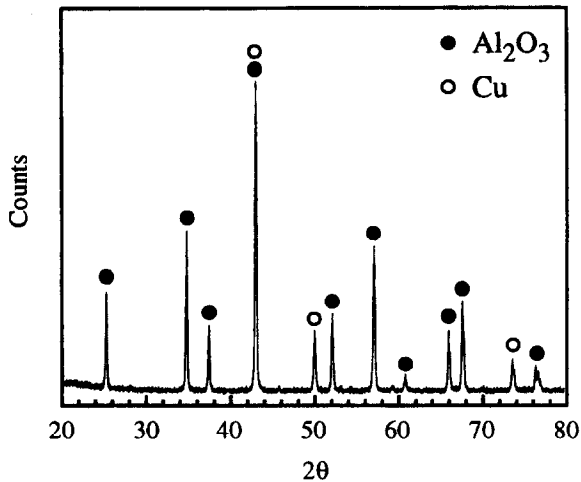


Fig. 2. XRD pattern of the powder mixture reduced at 1000°C in  $H_2$ .

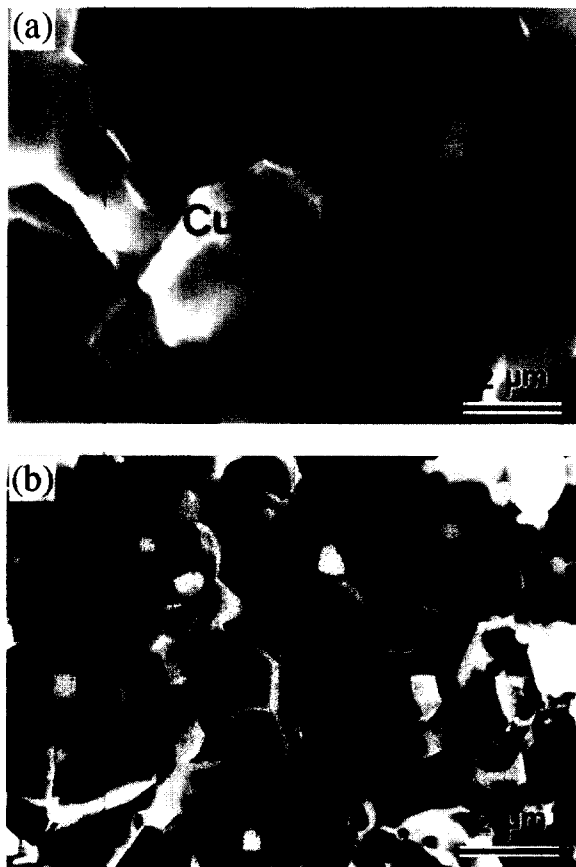


Fig. 3. Comparison of the fracture surface on the composites, hot-pressed at 1600°C using different starting powder mixtures: (a)  $Al_2O_3/Cu$  and (b)  $Al_2O_3/CuO$ .

Table 1 summarizes the properties of the hot-pressed composites depending on starting powder mixtures. The composite using  $Al_2O_3/CuO$  powder mixture as starting materials showed larger fracture strength and toughness than that of the composite using  $Al_2O_3/Cu$  powder mixture. These results indicated that the starting materials strongly influenced the microstructure and properties of composites, and thus the  $Al_2O_3/Cu$  composites

Table 1. Relative density and mechanical properties of  $Al_2O_3/5$  vol% Cu composites, hot-pressed at 1600°C for 1h

Powder mixture	$\rho_{th}(\%)$	$\sigma_f$ (MPa)	$K_{Ic}$ (MPa $\sqrt{m}$ )
$Al_2O_3/Cu$	97.1	$370 \pm 36$	$4.72 \pm 0.20$
$Al_2O_3/CuO$	98.1	$583 \pm 47$	$5.40 \pm 1.15$

with enhanced mechanical properties can be fabricated by using  $Al_2O_3/CuO$  powder mixture, more effectively.

### 3.3 Effect of hot-pressing temperatures

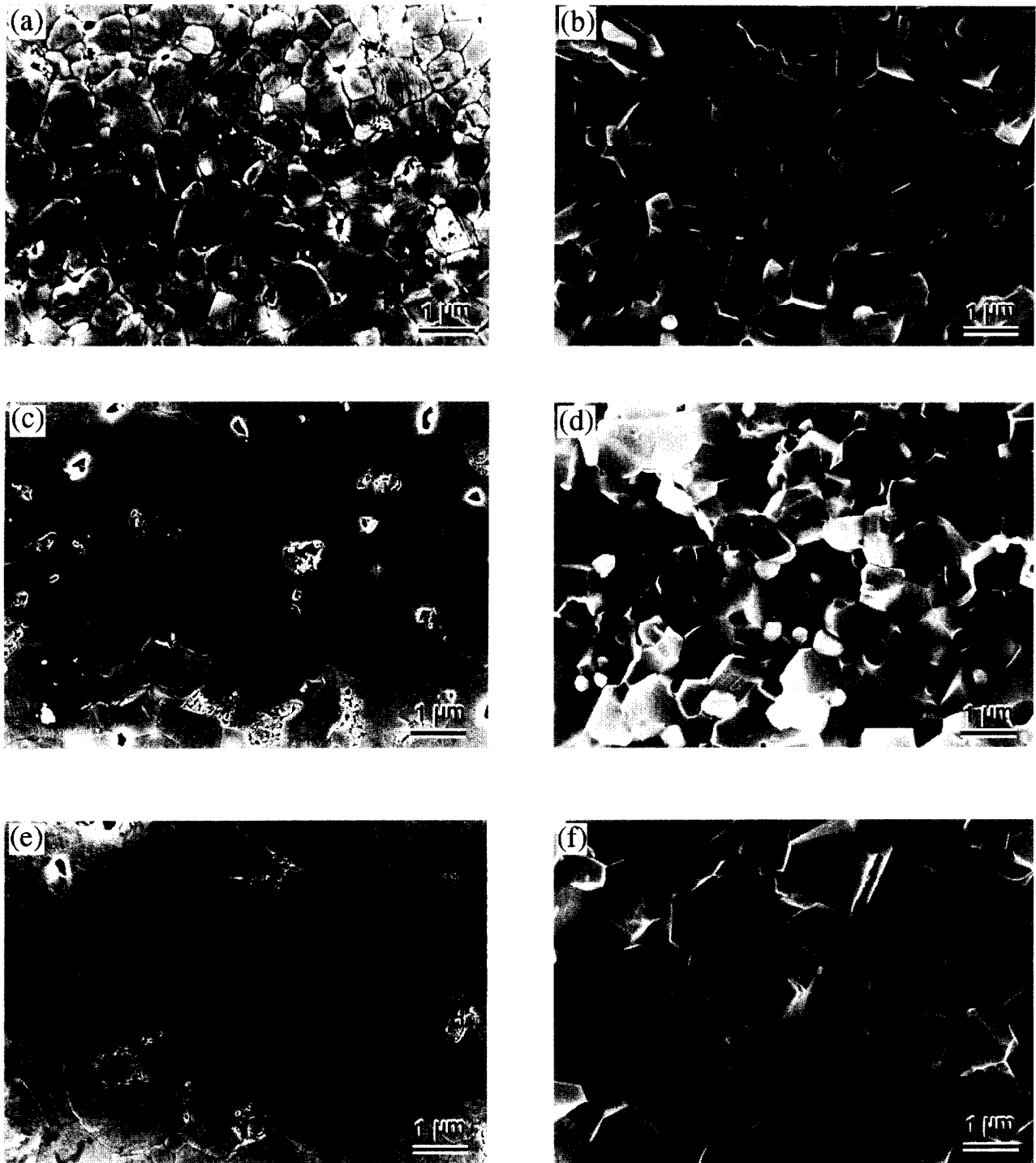
The effect of hot-pressing temperatures on mechanical properties was investigated in the composite using  $Al_2O_3/CuO$  powder mixture as starting materials. The powder mixtures were reduced at 350 and 1000°C for 30 min in  $H_2$  atmosphere, followed by the hot-pressing at 1400, 1450, 1500 and 1600°C for 1 h in Ar atmosphere under a pressure of 30 MPa, respectively. In all hot-pressed specimens the X-ray diffraction revealed only the Cu and  $Al_2O_3$  phase.

Figure 4 shows a typical TEM image of the composite hot-pressed at 1450°C. The Cu particles indicated by arrows were located mainly on  $Al_2O_3-Al_2O_3$  grain boundaries and triple points rather than within the  $Al_2O_3$  grains. The average particle size of Cu was approx. 200 nm. Hence, in this investigation the  $Al_2O_3/5$  vol% Cu composite is defined as an intergranular-type nanocomposite.<sup>2</sup>

Figure 5 shows polished and thermally etched (left) and fracture surfaces (right) of  $Al_2O_3/Cu$  nanocomposites hot-pressed at 1450 and 1500°C and of monolithic  $Al_2O_3$  at 1450°C, respectively. Increasing hot-pressing temperature to 1500°C resulted in an increase in matrix grain size and Cu-dispersoid size. A comparison of composite [Fig. 5(a)] with monolithic  $Al_2O_3$  [Fig. 5(e)], hot-pressed at the same temperature of 1450°C,



Fig. 4. Transmission electron micrographs for  $Al_2O_3/5$  vol% Cu nanocomposite, hot-pressed at 1450°C for 1h.



**Fig. 5.** Etched and fracture surfaces of the hot-pressed specimens observed in SEM. Composite at 1450°C: (a) etched, (b) fractured. Composite at 1500°C: (c) etched, (d) fractured. Monolithic alumina at 1450°C: (e) etched, (f) fractured.

revealed that the marked matrix grain refinement was achieved by the addition of 5 vol% Cu in the form of finely divided and uniformly distributed particles.

Figure 2 summarizes some properties of the monolithic  $\text{Al}_2\text{O}_3$  hot-pressed at 1450°C and  $\text{Al}_2\text{O}_3/5$  vol% Cu composites hot-pressed at various temperatures. The density was found to range from 99.4 to 98.1% of the theoretical density. Young's modulus of the composites exhibited the same value as 370 GPa in all hot-pressing temperature, while Young's modulus of monolithic

$\text{Al}_2\text{O}_3$  hot-pressed at 1450°C showed a value of 396 GPa. The lowered value in the composite could be explained by addition of ductile particles to the matrix.

The grain size variance of composites with hot-pressing temperature is also shown in Table 2. There is a progressive increase in grain size of composites with increasing hot-pressing temperature. In the comparison with monolithic  $\text{Al}_2\text{O}_3$  hot-pressed at 1450°C, the grain size of the composite was smaller, at 0.63  $\mu\text{m}$ , than that of  $\text{Al}_2\text{O}_3$  at 0.89  $\mu\text{m}$ . It is clear that the Cu particles significantly

**Table 2.** Properties of the monolithic alumina and Al<sub>2</sub>O<sub>3</sub>/5 vol% Cu composites

HP temp. (°C)	$\rho_{th}$ (%)	$E$ (GPa)	Grain size ( $\mu\text{m}$ )
1450*	99.2	396	0.89
1400	99.2	371	0.63
1450	99.3	370	0.63
1500	99.4	370	0.84
1600	98.1	369	1.37

\*Monolithic alumina.

inhibited grain growth of the Al<sub>2</sub>O<sub>3</sub> matrix, presumably by the pinning effect comprehensively described in the literature for composite systems containing the second phase.<sup>12</sup>

### 3.4 Mechanical properties

Dependence of the mechanical properties for the Al<sub>2</sub>O<sub>3</sub>/5 vol% Cu composites on hot-pressing temperature is shown in Table 3. Increasing hot-pressing temperature produced a decrease of hardness and increase of toughness. This change in hardness and toughness was thought to be due to the grain growth of the Al<sub>2</sub>O<sub>3</sub> matrix and coalescence of Cu-dispersoids which induced crack propagation with a large deflection.<sup>7</sup> A maximum strength value of 707 MPa was achieved in specimens hot-pressed at 1450°C, and increasing temperature to 1600°C caused the fracture strength to decrease to 583 MPa, which corresponded directly to the grain growth of Al<sub>2</sub>O<sub>3</sub> matrix shown in Table 2.

In comparison with monolithic Al<sub>2</sub>O<sub>3</sub>, the fracture strength and toughness of composite hot-pressed at 1450°C exhibited an enhanced value of 707 MPa and 4.28 MPa $\sqrt{\text{m}}$ , which were 1.3 times larger than that of the monolithic Al<sub>2</sub>O<sub>3</sub> prepared under the same conditions. From consideration of the measured grain size shown in Table 2, it is reasonable to expect the fracture strength to increase with decreasing grain size, as suggested by Petch for brittle metals, or by the Griffith criterion for brittle fracture.<sup>13</sup> The strengthening of Al<sub>2</sub>O<sub>3</sub>/Cu composites is, therefore, explained as being mainly due to the refinement of the Al<sub>2</sub>O<sub>3</sub> matrix.

The toughening mechanism believed to be effective in ceramic/metal composites is the plastic

stretching of metallic inclusions bridging the growing crack.<sup>14</sup> If the elastic modulus of the metal is lower than that of the ceramic matrix, i.e. the crack is attracted by the metallic particle, and if the metallic particles are firmly bonded to the brittle matrix which means that they should be kept below the critical size at which thermal mismatch stresses become sufficient to induce cracks, the contribution to the toughness of constrained particulate Cu-metal by the Al<sub>2</sub>O<sub>3</sub>-matrix could be calculated with the theoretical predictions of Ashby *et al.*<sup>15</sup>

$$\Delta K_{Ic} = E[CV_f \frac{\sigma_0}{E} d]^{1/2} \quad (2)$$

where  $\Delta K_{Ic}$  is the toughness increase,  $C$  is a constant which depends on the interfacial strength. The value of  $C = 1.6$ , for complete bonding with no matrix fracture, rises to as much as 6 with limited debonding or matrix fracture.  $E$  is the elastic modulus of Cu,  $V_f$  is the area fraction on the crack plane (equivalent to the volume fraction of the metallic particles),  $\sigma_0$  is the initial flow stress at yield strain of the metal particle in uniaxial tension (scaling with yield stress of Cu, 78 MPa)<sup>16</sup> and  $d$  is the particle diameter (200 nm, in composite hot-pressed at 1450°C). Using the data in Table 4,<sup>16,17</sup>  $\Delta K_{Ic}$  is calculated to be 0.29 MPa $\sqrt{\text{m}}$  for the complete bonding of particle with no matrix fracture and to be 0.56 MPa $\sqrt{\text{m}}$  for the limited debonding or matrix fracture.

From microstructural observation of the interactions between the crack and the Cu particles shown in Fig. 6, the crack may either propagate along the interface, or bypass the bridging particle. It allows the experimental results to be compared with the theoretical predictions of eqn (2). However, toughness increase by theoretical calculation displayed a lower value than that by experimental result, i.e. 0.71 MPa $\sqrt{\text{m}}$  in composite hot-pressed at 1450°C. Furthermore, it was reported in Ni particulate reinforced Al<sub>2</sub>O<sub>3</sub> composite system that the constant  $C$  in eqn (2) showed smaller value than that predicted by Ashby *et al.*, as 0.24–1.8.<sup>18</sup> If this constant is taken into consideration for theoretical calculation in the Al<sub>2</sub>O<sub>3</sub>-Cu system, the fracture toughness predicted by the present model would be smaller.

**Table 3.** Dependence of the mechanical properties on hot-pressing temperatures

HP temp. (°C)	$HV^{\dagger}$ (GPa)	$K_{Ic}$ (MPa $\sqrt{\text{m}}$ )	$\sigma_f$ (MPa)
1450*	17.8	3.57 ± 0.25	536 ± 35
1400	17.2	3.65 ± 0.26	668 ± 46
1450	17.0	4.28 ± 0.35	707 ± 45
1500	16.5	4.45 ± 0.25	668 ± 55
1600	15.5	5.40 ± 1.15	583 ± 47

\*Monolithic alumina. <sup>†</sup>Vickers hardness at 10 kg load.**Table 4.** Material properties of Al<sub>2</sub>O<sub>3</sub> and Cu

Property	Al <sub>2</sub> O <sub>3</sub>	Cu
Density (g cm <sup>-3</sup> )	3.98	8.94
Young's modulus (GPa)	390	130
Poisson's ratio	0.220	0.343
Volume fraction	0.95	0.05
CTE ( $\times 10^{-6}$ °C <sup>-1</sup> )*	8	17

\*Coefficient of thermal expansion of 0–100°C.

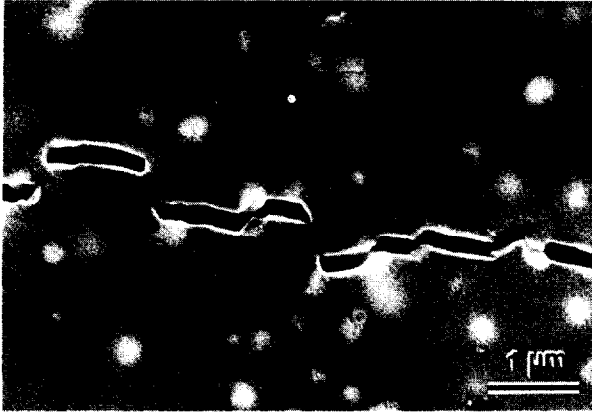


Fig. 6. Typical microstructure of Al<sub>2</sub>O<sub>3</sub>/Cu composite, hot-pressed at 1450°C for 1h and the cracks introduced by indentation.

Thus, in addition to the toughening by crack bridging, another factor that may affect the increase in toughness of the composite may be considered. A possible mechanism is toughening by the thermal residual stress field due to the mismatch of coefficients of thermal expansion (CTE) between the matrix and the particulates as the composite was cooled to room temperature.<sup>19</sup> On the basis of this mechanism, the change in  $K_{Ic}$  can be expressed in the following form:<sup>19,20</sup>

$$\Delta K_{stress} = 2\bar{\sigma}\sqrt{\frac{2\lambda}{\pi}} \quad (3)$$

where  $\bar{\sigma}$  is the mean stress acting over regions of compression, and the wavelength of the stress field is  $\lambda$ . However, it was expected from easy stress relaxation due to the low melting temperature (1084°C) and yield stress (78 MPa) of Cu that mean thermal residual stress ( $\bar{\sigma}$ ) would be small.<sup>20</sup> The predicted toughness increase based on the model described by Taya *et al.*<sup>21</sup> indeed showed a small amount, 0.1 MPa√m for  $\Delta T = 1000^\circ\text{C}$ . Thus, in the Al<sub>2</sub>O<sub>3</sub>/Cu composite system, it appears that this mechanism might have only a minor effect on increase in toughness, though it cannot be completely ruled out.

Conversely, the mechanical properties of Cu used in our analysis were taken from Ref. 16, where yield stress was listed as 78 MPa for the 99.99% purity and not deformed state. But if the Cu could be heavily deformed during cooling (increase of yield stress), it may follow from eqn (2) that  $\Delta K_{Ic}$  is directly increased. Hence, it strongly suggests that further analyses need to be undertaken on the composite, including precise microstructural characterizations by TEM, to confirm the Cu state in the hot-pressed composite.

Finally, though it is difficult to conclude which mechanism plays an important role in toughening of Al<sub>2</sub>O<sub>3</sub>/Cu nanocomposite, the SEM microstructure for crack propagation shown in Fig. 6, and theoretical prediction, suggest that the major portion of observed toughness increase in the present composite is attributable to toughening due to crack bridging.

#### 4 Conclusions

Two methods for the preparation of initial powder mixture for fabrication of Al<sub>2</sub>O<sub>3</sub>/5 vol% Cu nanocomposite have been presented and discussed on the basis of microstructural features and mechanical properties. Al<sub>2</sub>O<sub>3</sub>/5 vol% Cu nanocomposite fabricated by the reduction and sintering method using Al<sub>2</sub>O<sub>3</sub> and CuO powder mixture showed marked refinement of Al<sub>2</sub>O<sub>3</sub> grain size and homogeneous distribution of Cu, with an average size of 200 nm.

Mechanical properties of composites were investigated as a function of hot-pressing temperature. These data indicate that maximum strengthening of 707 MPa, which is much higher than that of Al<sub>2</sub>O<sub>3</sub>, at 536 MPa, are obtained at the hot-pressing temperature of 1450°C. The toughness increase is explained by the crack bridging and compressive thermal residual stress. The strengthening is mainly attributed to the toughness improvement and the refinement of matrix grains by the nano-sized Cu dispersion at the grain boundary.

#### Acknowledgements

The authors wish to thank Yong-Ho Choa for helpful discussions. They are further grateful to Jai-Sung Lee and Ji-Hun Yu of the Hanyang University in Korea for his interest in this work and for assistance in preparation of hygrometry measurements.

#### References

1. Niihara, K., Nakahira, A., Sasaki G. and Hirabayashi, M., Development of strong Al<sub>2</sub>O<sub>3</sub>/SiC composites. In *Proceedings of the First MRS International Meeting on Advanced Materials*, Vol. 4, eds M. Doyama, S. Somiya and R. P. H. Chang. Materials Research Society, Pittsburgh, PA, 1989, pp. 129–134.
2. Niihara, K., New design concept of structural ceramics—ceramic nanocomposite. *Journal of the Ceramic Society of Japan*, 1991, **99**, 974–982.
3. Niihara, K., Nakahira, A. and Sekino, T., New nano-composite structural ceramics. *Materials Research Society Symposium Proceedings*, 1993, **286**, 405–412.
4. Niihara, K., Sekino, T. and Nakahira, A., Ceramic based nanocomposites with improved properties and new

- functions. In *New Functionality Materials*, Vol. C, eds T. Tsuruta and M. Doyama and M. Seno. Elsevier Science, Tokyo, 1993, pp. 751–756.
5. Brook, R. J. and Mackenzie, R. A. D., Nanocomposite materials. *Materials World*, 1993, **1**, 27–30.
  6. Sekino, T. and Niihara, K., Microstructural characteristics and mechanical properties for  $Al_2O_3$ /metal nanocomposites. *Nanostructured Materials*, 1995, **6**, 663–666.
  7. Nawa, M., Sekino, T. and Niihara, K., Fabrication and mechanical behaviour of  $Al_2O_3/Mo$  nanocomposites. *Journal of Materials Science*, 1994, **29**, 3185–3192.
  8. Sekino, T., Nakajima, T. and Niihara, K., Mechanical and magnetic properties of nickel dispersed alumina-based nanocomposites. *Materials Letters*, 1996, **29**, 165–169.
  9. Nawa, M., Yamazaki, K., Sekino, T. and Niihara, K., A new type of nanocomposite in tetragonal zirconia polycrystal–molybdenum system. *Materials Letters*, 1994, **20**, 299–304.
  10. Hyuga, H., Hayashi, Y., Sekino, T. and Niihara, K., Fabrication process and electrical properties of  $BaTiO_3/Ni$  nanocomposites. *Nanostructured Materials*, 1997, **9**, 547–550.
  11. *Gmelins Handbuch der Anorganischen Chemie*, Cu. 8. Aufl., System-Nummer 60. Verlag Chemie GmbH, Weinheim, 1958, pp 84–85.
  12. Smith, C. S., Grains, phase and interphases: an interpretation of the microstructure. *Transactions of the Metallurgical Society AIME*, 1948, **175**, 15–51.
  13. Kingery, W. D., Bowen, H. K. and Uhlmann, D. R., *Introduction to Ceramics*, 2nd edn. John Wiley and Sons, New York, 1976, pp. 765–815.
  14. Budiansky, B., Amazigo, J. C. and Evans, A. G., Small-scale crack bridging and the fracture toughness of particulate-reinforced ceramics. *Journal of the Mechanics and Physics of Solids*, 1988, **36**, 167–187.
  15. Ashby, M. F., Blunt, F. J. and Bannister, M., Flow characteristics of highly constrained metal wires. *Acta metallurgica*, 1989, **37**, 1847–1857.
  16. Smithells, C. J., *Metals Reference Book*. 5th edn. Butterworths, London, 1976.
  17. Touloukian, Y. S., *Thermophysical Properties of High Temperature Solid Materials*. Vol. 6. Macmillan Co., New York, 1973.
  18. Tuan, W. H. and Brook, R. J., The toughening of alumina with nickel inclusions. *Journal of the European Ceramic Society*, 1990, **6**, 31–37.
  19. Evans, A. G., Heuer, A. H. and Porter, D. L., The fracture toughness of ceramics. In *Fracture 1997, Advances in Research on the Strength and Fracture of Materials, Fourth International Conference on Fracture*, Vol. 1, ed. D. M. R. Taplin. Pergamon, New York, 1978, pp. 529–556.
  20. Cutler, R. A. and Virkar, A. V., The effect of binder thickness and residual stresses on the fracture toughness of cemented carbides. *Journal of Materials Science*, 1985, **20**, 3557–3573.
  21. Taya, M., Hayashi, S., Kobayashi, A. S. and Yoon, H. S., Toughening of a particulate-reinforced ceramic-matrix composite by thermal residual stress. *Journal of the American Ceramic Society*, 1990, **73**, 1382–1391.